Supporting information for

A >200 meV uphill thermodynamic landscape for radical transport in *E. coli* ribonucleotide reductase determined using fluorotyrosine-substituted enzymes

Kanchana R. Ravichandran[†], Alexander T. Taguchi[†], Yifeng Wei[†], Cecilia Tommos[§], Daniel G. Nocera[⊥,], JoAnne Stubbe[†,‡,*]*

[*]To whom correspondence should be addressed: dnocera@fas.harvard.edu, stubbe@mit.edu

[†] Department of Chemistry and [‡] Department of Biology, Massachusetts Institute of Technology, 77 Massachusetts Avenue, Cambridge, MA 02139, United States

[§] Department of Biochemistry and Biophysics, University of Pennsylvania, Philadelphia, PA 19104, United States

[⊥] Department of Chemistry and Chemical Biology, Harvard University, 12 Oxford Street, Cambridge, MA 02138, United States

SUPPORTING INFORMATION TABLE OF CONTENTS

Detailed description of data analysis using Method B. Data analysis by Method B is demonstrated here for one trial of the temperature-dependent EPR studies of the reaction of F_3Y_{122}•-β2 with Y_{731}F-α2, CDP and ATP. In the first step, a baseline correction was performed using the regions of the spectrum where no signal is expected (g-values < 1.955 and > 2.051). A second order polynomial function of the form $ax^2 + bx + c$ was found to be sufficient to correct for the slight curvature of the baseline in the EPR spectra. Without this baseline correction, a systematic reduction in the calculated percentage of Y_{356}• spectra from 0 to 3% was observed (see Table S1 and S2 under Method B).

In the second step, 0.5 equiv of the total F_3Y_{122}•-β2 was subtracted from each EPR spectrum using the F_3Y_{122}•-β2 reference spectrum.[1] The resulting composite spectra show the interconversion between F_3Y_{122}• and Y_{356}• as a function of temperature, free from the complications associated with half sites reactivity (Figure S1A-B). This subtraction decreases the S/N level of the spectra such that the relative amounts of F_3Y_{122}• and Y_{356}• cannot be reliably determined by eye (Figure S1C). Therefore, a script was written in Matlab 2016a to subtract the remaining F_3Y_{122}• determined by adjusting the intensity of the F_3Y_{122}•-β2 reference spectrum until the least-squares difference between the reference spectrum and the composite spectrum in the g-value interval between 2.0363 to 2.0390 (this defines the highest S/N region of the low-field F_3Y_{122}• features) was minimized (Figure S1C). The amount of Y_{356}• after subtraction of the remaining F_3Y_{122}• was determined by double integration. The Y_{356}• spectrum determined by this method shown in Figure S1D is the same in each sample, supporting the robustness of the method.

Total spin determination: Methods A and B. The total spin of the EPR spectra was checked by double integration to ensure that Methods A and B were not biased by spin loss artifacts. No significant spin loss was observed in any of the samples. Less than a 3% variation in the total spin was determined from EPR spectra of samples that had undergone freeze-thaw cycles at 25 °C, 2 °C, and then back to 25°C (Table S3).

TABLE S1. Temperature dependence of Y_{356}• formation: hand-quench (HQ) vs rapid freeze-quench (RFQ).

Temperature (°C)	HQ-Method A (% Y_{356}• of total spin)	HQ-Method B (% Y_{356}• of total spin)	RFQ-Method A (%Y_{356}• of total spin)
2	13 ± 2	17 ± 5	19
5	16 ± 2	21 ± 1	30
8	21 ± 1	24 ± 1	-
10	24 ± 1	31 ± 4	36
12	22 ± 2	28 ± 1	-
15	27 ± 1	31 ± 2	37
20	28 ± 3	34 ± 4	43
25	29 ± 3	34 ± 5	41
30	33 ± 4	37 ± 3	42
37	33 ± 2	33 ± 1	40

The HQ data represent the averages of three independent trials. The RFQ data represent a single trial. Analysis methods A and B are described in the main text.

TABLE S2. The pH dependence of Y_{356}• formation.

pH	5 °C-Method A	5 °C-Method B	25 °C-Method A	25 °C-Method B
6.8	-[a]	4 ± 1	5 ± 2	9 ± 1
7.0	5[b]	6 ± 2	12 ± 1	14 ± 2
7.2	10 ± 2	10[b]	19 ± 1	30 ± 5
7.4	14 ± 4	18 ± 2	25 ± 2	36 ± 3
7.6	18[b]	18 ± 4	31[b]	35 ± 5
7.8	25 ± 2	28 ± 6	35[b]	42 ± 2
8.0	26 ± 3	31 ± 6	38 ± 3	43 ± 1

The numbers represent percentage Y_{356}• of total spin. Analysis methods A and B are described in the main text.

[a] Y_{356}• amount was < 3%.

[b] The two trials provided the same quantitation.

TABLE S3. Temperature dependent equilibration of F_3Y_{122}• and Y_{356}• in the reaction of F_3Y_{122}•-β2, CDP, ATP and Y_{731}F-α2 or Y_{730}F-α2.

α2 mutant	25 °C → 2 °C → 25 °C (% Y_{356}• of total spin)
Y_{731}F	35 → 16 → 30
Y_{730}F	26 → 12 → 30

The reaction mixture was incubated at 25 °C, frozen in liquid isopentane and analyzed by EPR spectroscopy. This same sample was subject to freeze-thaw cycles and analyzed at 2 °C and again, at 25 °C. No total spin loss was recorded with the freeze-thaw cycles. The composite spectra of each reaction are shown in Figure S7.

TABLE S4. Hyperfine values (MHz) for β-^{1}H and ^{19}F of F_2Y• at different positions on pathway.

Position	Nucleus	A_{xx}	A_{yy}	A_{zz}
F_2Y_{122}•[a]	β-^{1}H	52	50	56
	^{19}F	9	16	157
F_2Y_{730}•[b,c]	β-^{1}H	63	63	63
	^{19}F	-15	-3	151
F_2Y_{731}•[b,c]	β-^{1}H	40	40	40
	^{19}F	-15	-3	157
F_2Y_{356}•[b,d]	β-^{1}H	54	52	54
	^{19}F	-15	-3	147

[a] Reference 1 and 2.

[b] The intrinsic EPR linewidth of 17 MHz was used. The hyperfine values for 2,6-^{1}H and one of the two β-^{1}H are significantly smaller than the EPR linewidth and were not included in the simulations.

[c] *g*-values of 2.0063, 2.0044 and 2.0022 were used. The simulation parameters were taken from reference 3.

[d] *g*-values of 2.0073, 2.0044 and 2.0022 were used.[3]

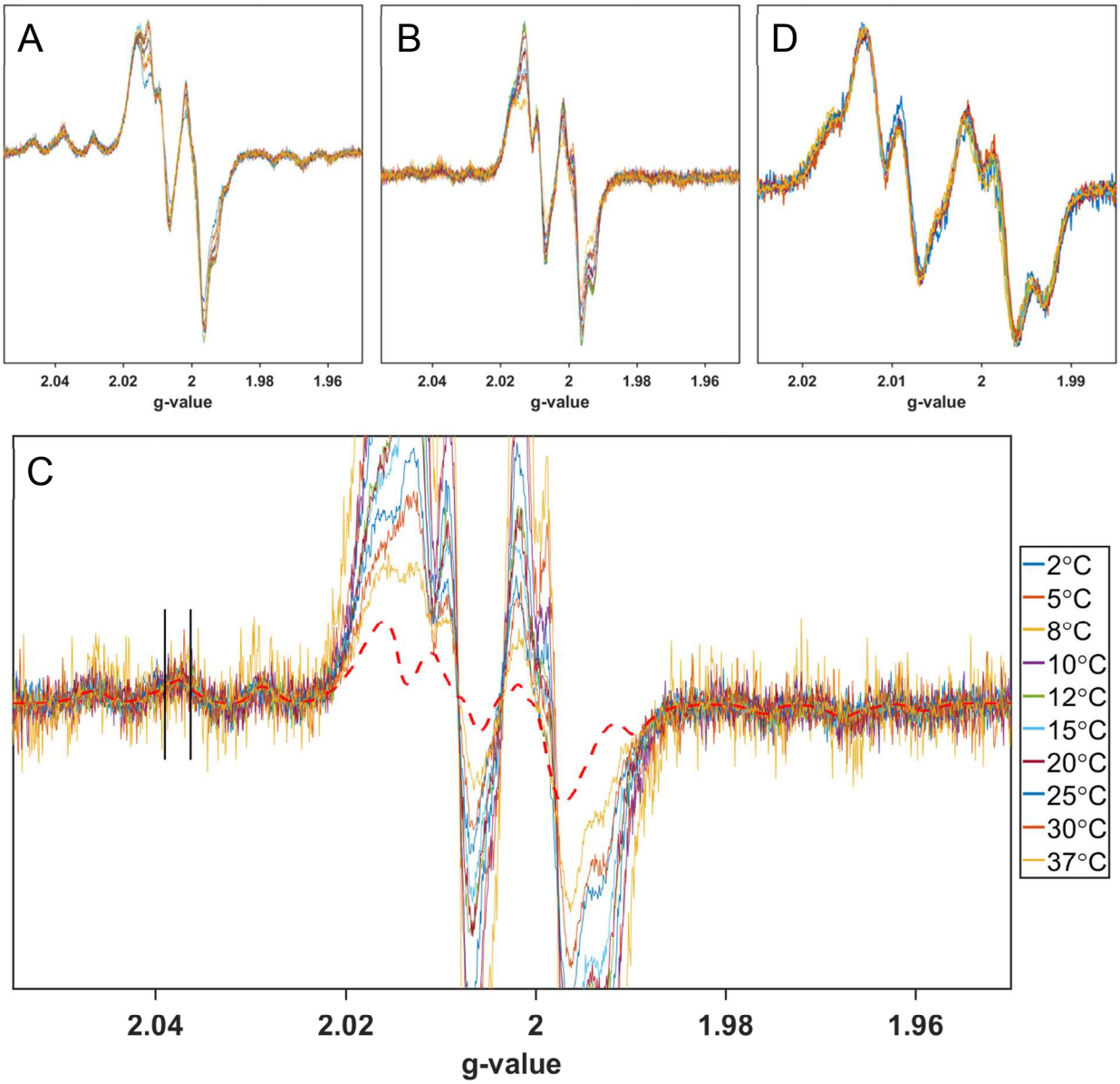

Figure S1. Analysis by Method B (main text) is described for one experiment in which the equilibration of the reaction mixture generated when F_3Y_{122}•-β2 is incubated with Y_{731}F-α2, CDP, and ATP as a function of temperature is examined. (A) Composite spectra before subtraction of nonreacting F_3Y_{122}•. (B) Composite spectra after subtracting the nonreacting F_3Y_{122}• which shows the interconversion between F_3Y_{122}• and Y_{356}• as a function of temperature. (C) Least-squares fitting of the F_3Y_{122}•-β2 reference spectrum (red dashed line) to the composite spectra in the g-value range 2.0363 to 2.0390 (marked by two vertical black lines). (D) Overlay of Y_{356}• spectra generated after subtraction of the remaining F_3Y_{122}• in (C) at different temperatures. The intensities of the spectra were normalized for visual comparison. At 2 °C (blue trace) the spectrum is slightly distorted relative to the other difference spectra. This observation is likely a consequence of the lower amount of Y_{356}• signal at this temperature.

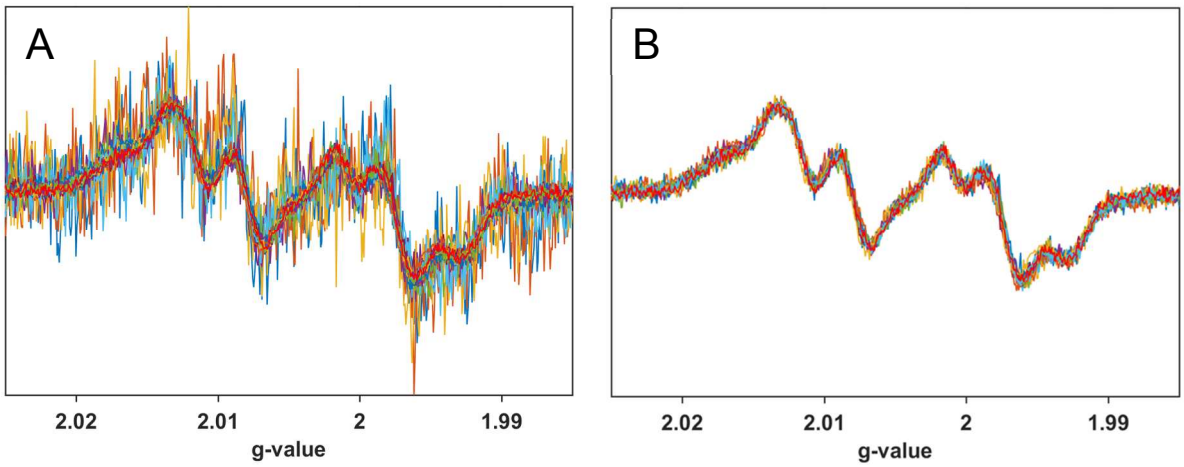

Figure S2. Analysis by Method B (main text) for the equilibration of the reaction mixture generated when F_3Y_{122}•-β2 is incubated with $Y_{731}F$-α2, CDP, and ATP as a function of pH at 25 °C. (A) All spectra from pH 6.8 to 8.0 are included. (B) Only spectra from pH 7.2 to 8.0 are included as the level of the Y_{356}• at the low pHs are very low.

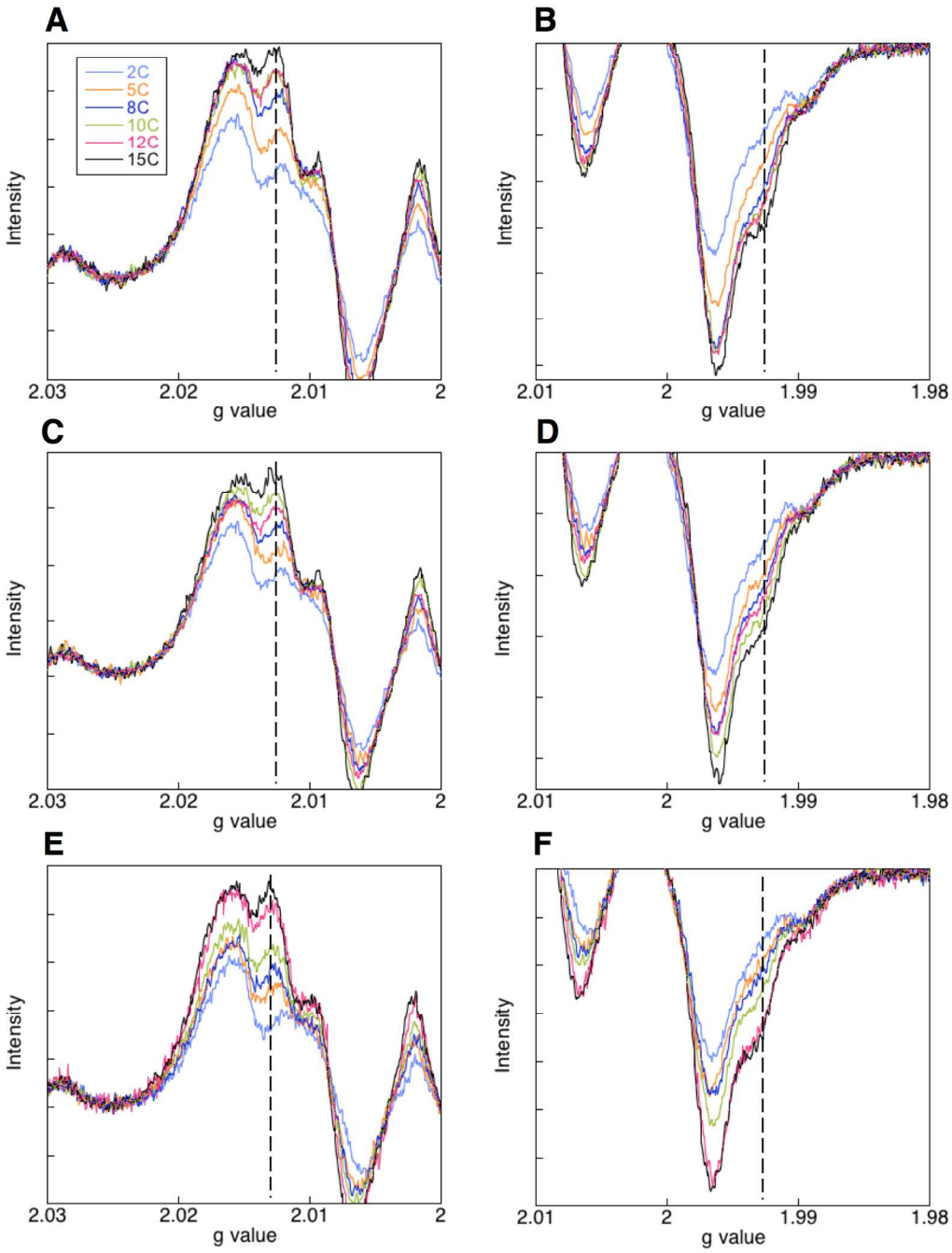

FIGURE S3. Composite EPR spectra of the F_3Y_{122}•-β2/Y_{731}F-α2/CDP/ATP reaction as a function of temperature (2–15 °C). The composite spectrum at each temperature was acquired on three independently prepared samples. The low- and high-field regions of the spectra for trial 1 (A and B), trial 2 (C and D) and trial 3 (E and F) are shown. The color code is described in panel A. The dotted lines identify spectral features that are characteristic of Y_{356}•. Trial 1 is also shown in Figure 3 of the main text.

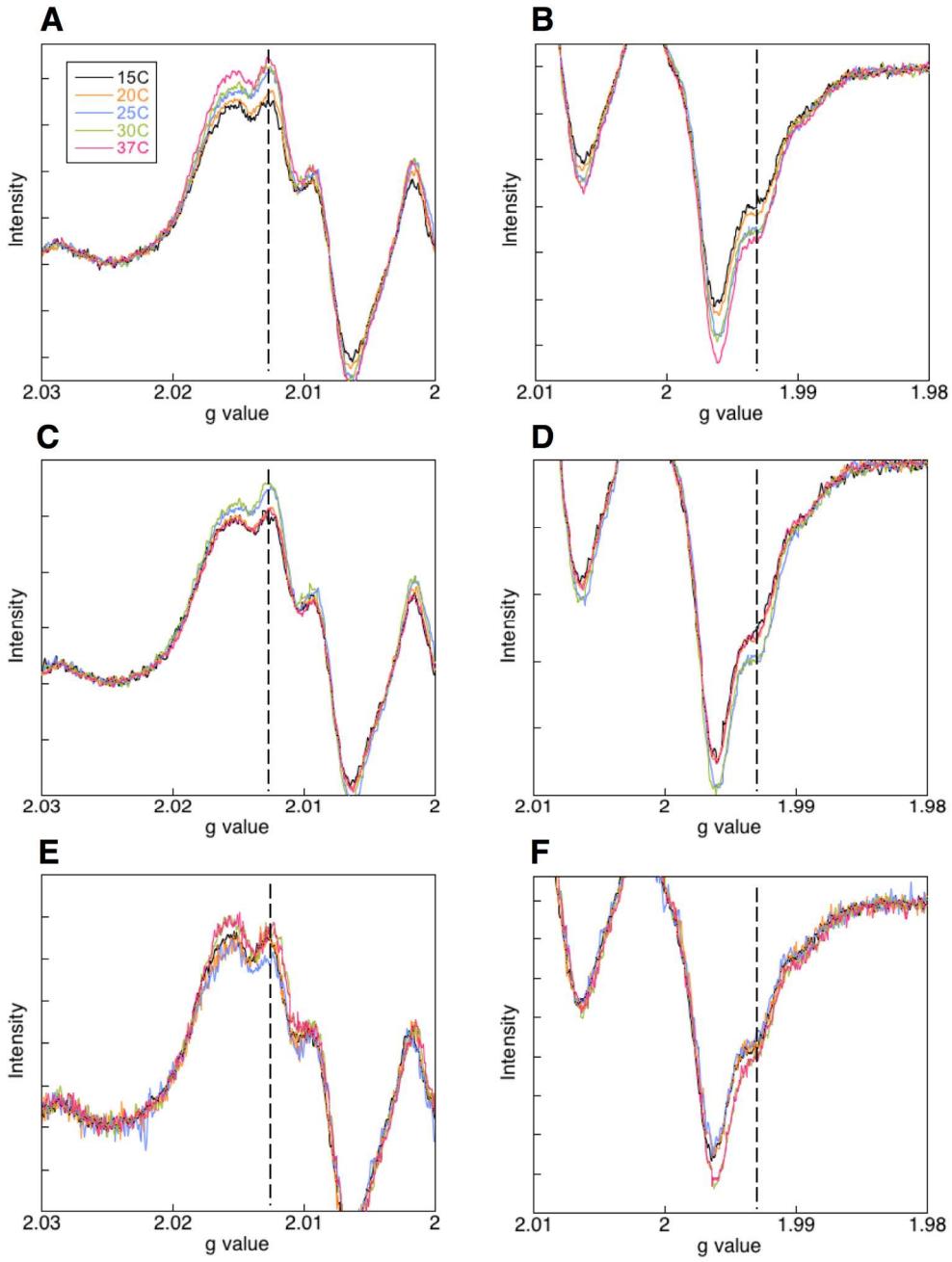

FIGURE S4. Composite EPR spectra of the F_3Y_{122}•-β2/Y_{731}F-α2/CDP/ATP reaction as a function of temperature (15–37 °C). The composite spectrum at each temperature was acquired on three independently prepared samples. The low- and high-field regions of the spectra for trial 1 (A and B), trial 2 (C and D) and trial 3 (E and F) are shown. The color code is described in panel A. The dotted lines identify spectral features that are characteristic of Y_{356}•.

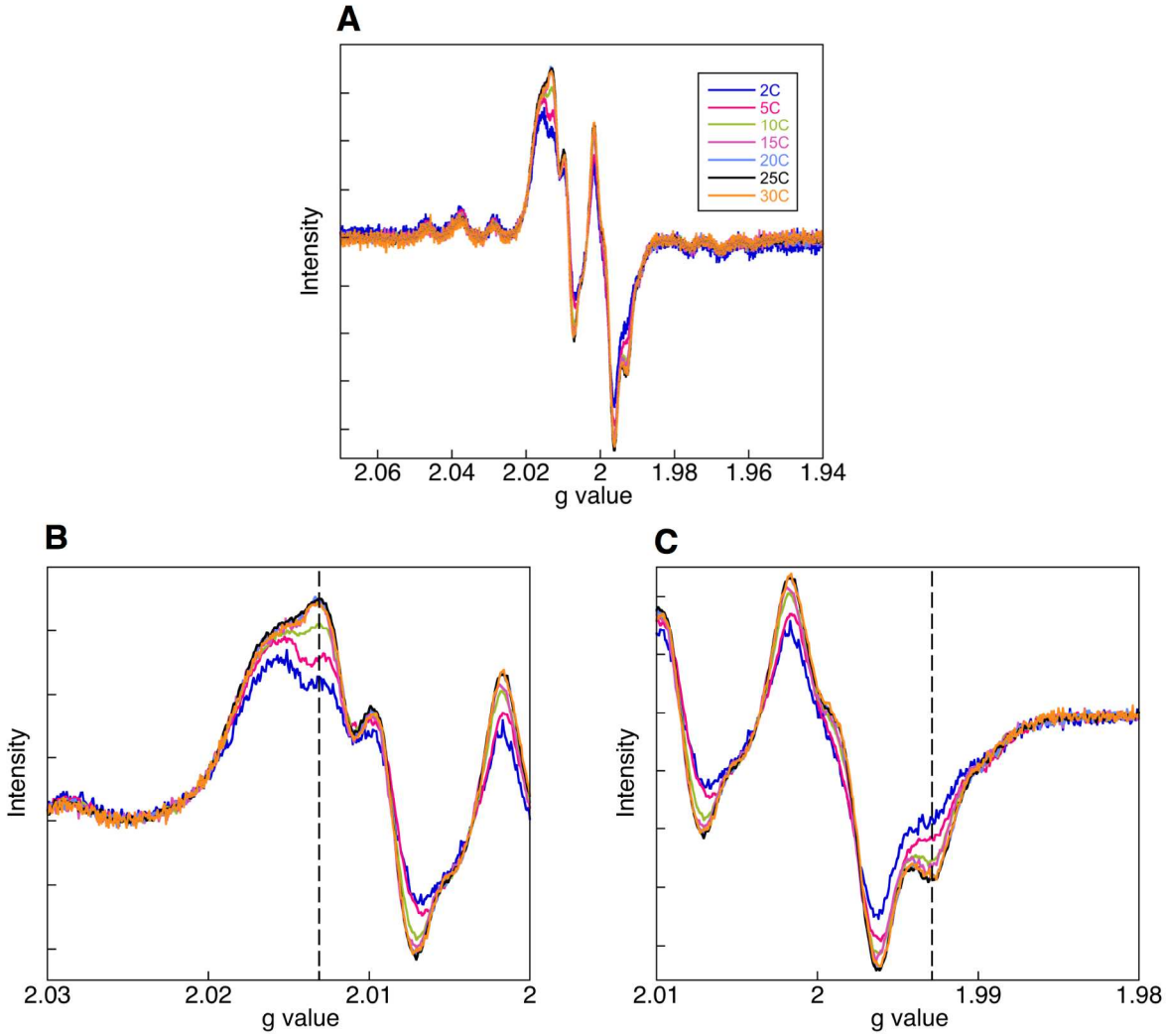

FIGURE S5. Temperature dependence of Y_{356}• formation monitored by RFQ-EPR spectroscopy. The composite EPR spectra recorded upon reacting F_3Y_{122}•-β2 (0.8 F_3Y•/β2, final concentration 35 μM), Y_{731}F-α2 (35 μM), CDP (1 mM) and ATP (3 mM) are shown in A. B and C. Expanded views of the low- and high-field regions of the spectra respectively. The color code is described in panel A.

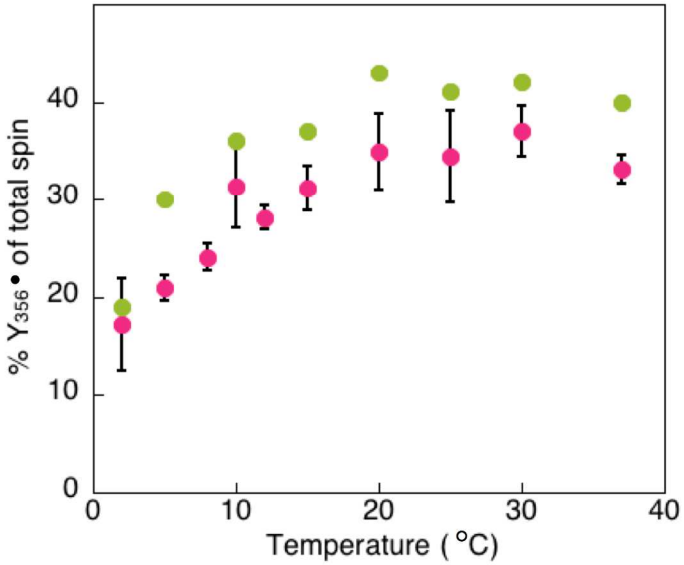

FIGURE S6. Temperature dependence of Y_{356}• formation in the reaction of F_3Y_{122}•-β2/Y_{731}F-α2/CDP/ATP as determined by HQ- and RFQ-EPR spectroscopies. The HQ data points (pink dots) represent the averages of three independent trials. The RFQ data points (green dots) represent a single trial.

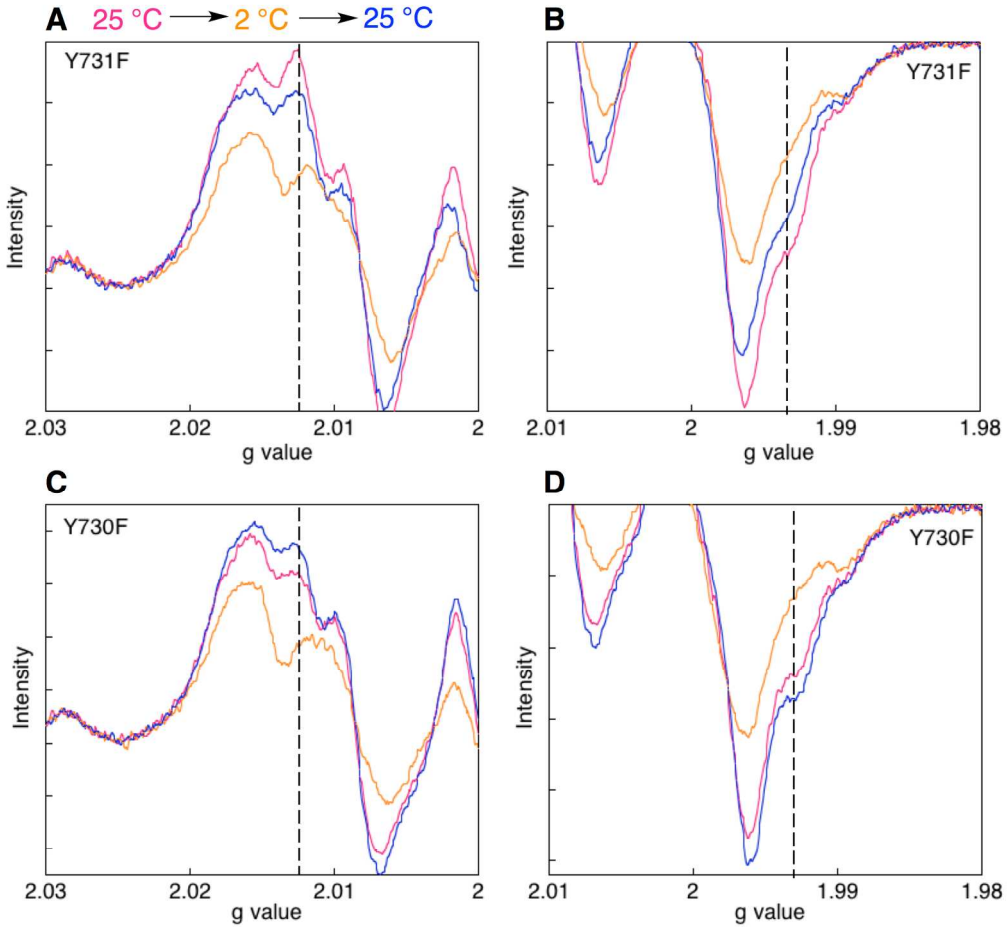

FIGURE S7. Temperature dependent equilibration of F_3Y_{122}• and Y_{356}• in the reaction of F_3Y_{122}•-β2, CDP, ATP and Y_{731}F-α2 or Y_{730}F-α2. Expanded views of the low- and high-field regions of the spectra for Y_{731}F-α2 (A and B) and Y_{730}F-α2 (C and D). The color code is described in panel A. In each case, the reaction was initiated at 25 °C and the spectrum was recorded (pink). The sample was subsequently thawed, incubated in a water bath set at 2 °C and re-frozen for EPR analysis (orange). The reaction mixture was thawed a third time, incubated in a 25 °C water bath and re-frozen for EPR analysis (blue). The percentage Y_{356}• for each spectrum is shown in Table S3. No spin loss was recorded during the freeze-thaw cycles.

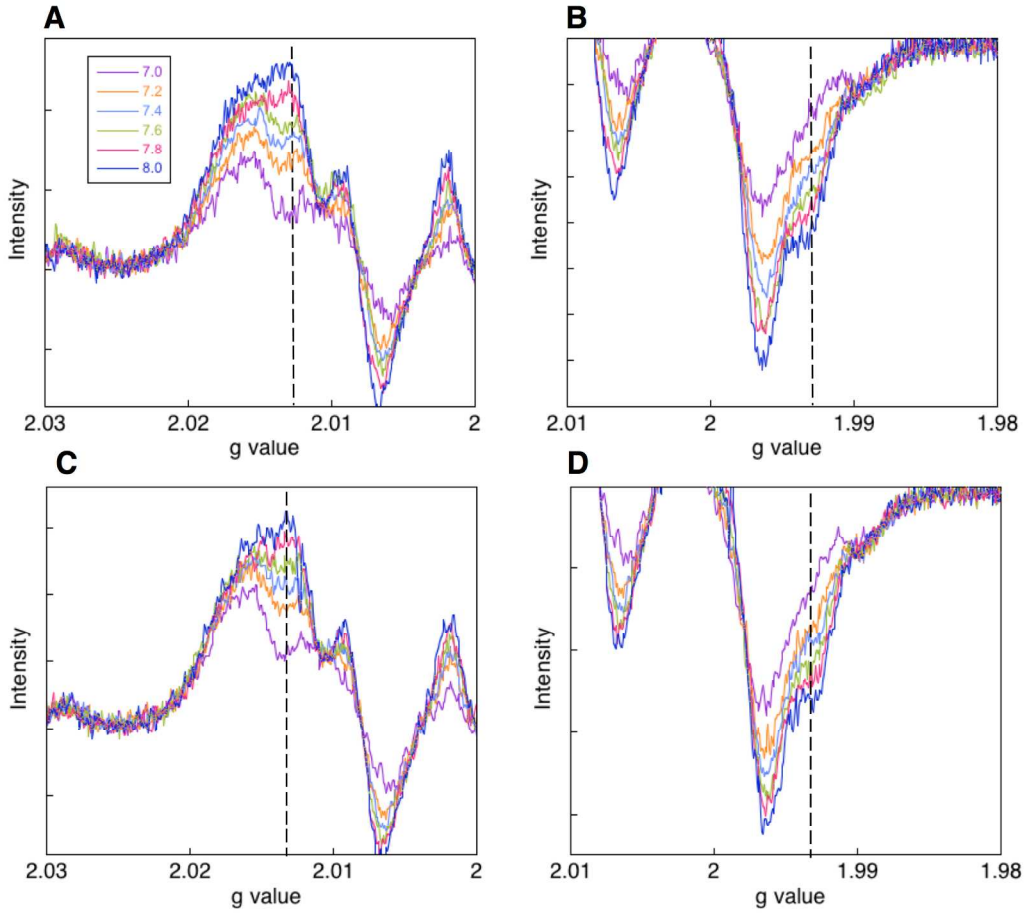

FIGURE S8. Composite EPR spectra of the F_3Y_{122}•-β2/Y_{731}F-α2/CDP/ATP reaction at 25 °C as a function of pH. The composite spectrum at each pH was acquired on two independently prepared samples. The low- and high-field regions of the spectra for trial 1 (A and B) and trial 2 (C and D) are shown. The colors represent different pH values as described in panel A. The dotted lines identify spectral features that are characteristic of Y_{356}•. Trial 1 is reproduced from the main text (Figure 5).

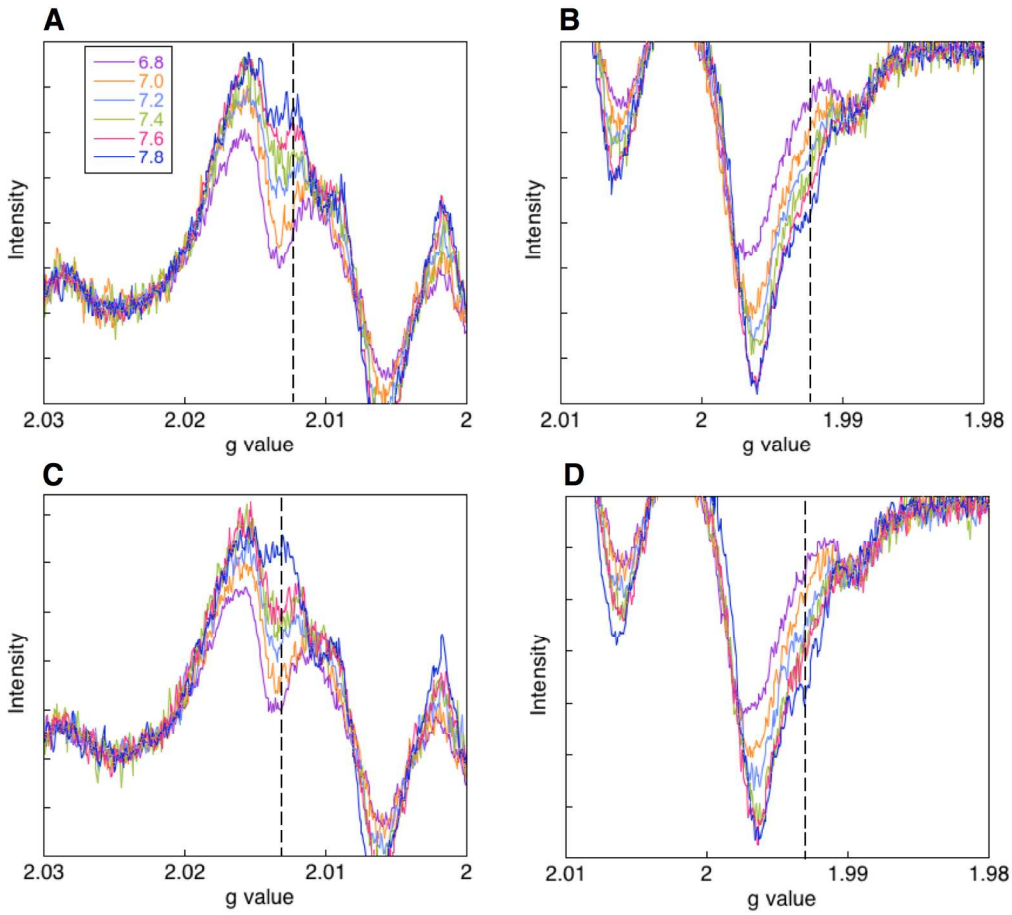

FIGURE S9. Composite EPR spectra of the F_3Y_{122}•-β2/Y_{731}F-α2/CDP/ATP reaction at 5 °C as a function of pH. The composite spectrum at each pH was acquired on two independently prepared samples. The low- and high-field regions of the spectra for trial 1 (A and B) and trial 2 (C and D) are shown. The colors represent different pH values as described in panel A. The dotted lines identify spectral features that are characteristic of Y_{356}•.

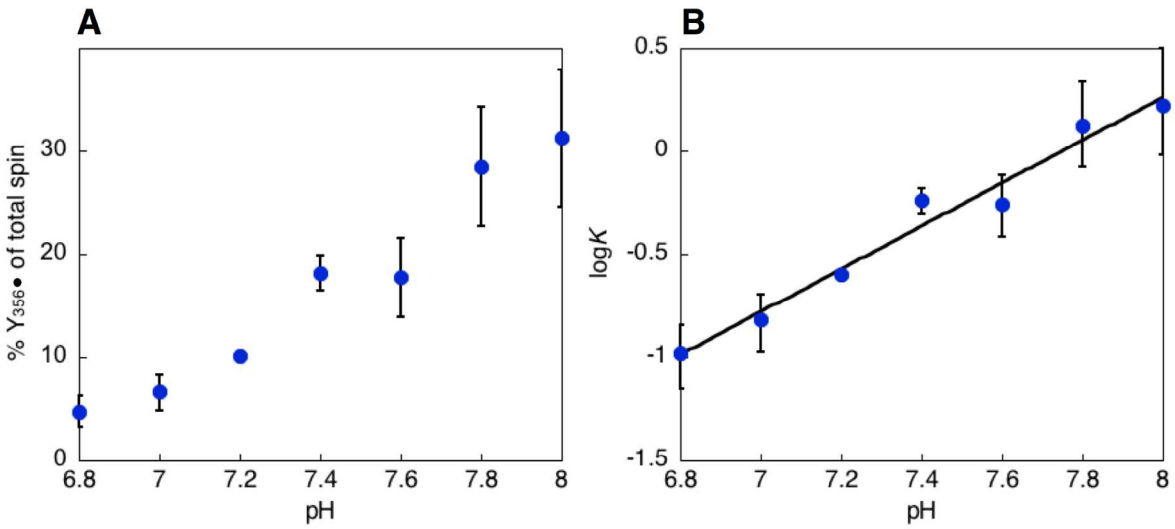

FIGURE S10. The pH dependence of Y_{356}• formation in the reaction of F_3Y_{122}•-β2/Y_{731}F-α2/CDP/ATP at 5 °C. A. Percentage Y_{356}• of total spin as a function of pH. B. The log*K* as a function of pH where *K* is the ratio of Y_{356}• to F_3Y_{122}•. The observed pH dependence of slope 1.0 ± 0.1 supports that the Y_{356}• proton is in fast exchange with solvent.

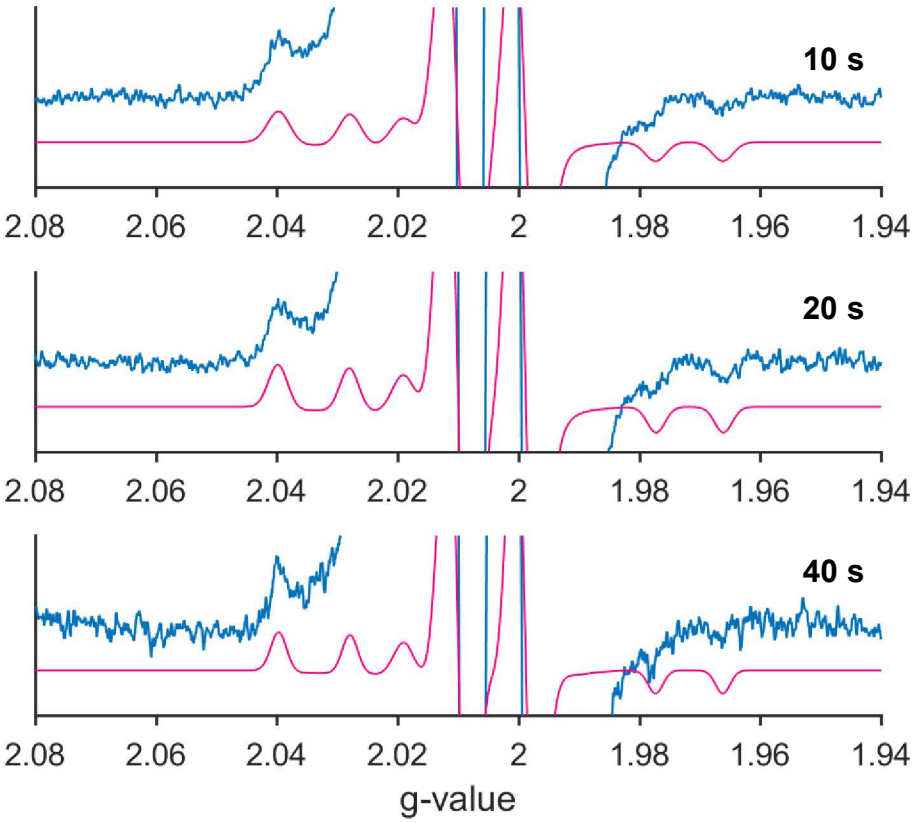

FIGURE S11. Reaction of F_2Y_{356}-β2, $Y_{731}F$-α2, CDP and ATP monitored by RFQ-EPR spectroscopy. An expanded view of the composite spectra recorded at the indicated time points shows wing features that are assigned to F_2Y_{356}•. The pink trace in each panel represents the simulated spectrum of F_2Y_{356}• using the parameters shown in Table S4. The 20 s data set is also reproduced in the main text (Figure 7).

REFERENCES

(1) Minnihan, E. C.; Young, D. D.; Schultz, P. G.; Stubbe, J. *J. Am. Chem. Soc.* **2011**, *133*, 15942-5.

(2) Oyala, P. H.; Ravichandran, K. R.; Funk, M. A.; Stucky, P.; Stich, T. A.; Drennan, C. L.; Britt, R. D.; Stubbe, J. *J. Am. Chem. Soc.* **2016**, *138*, 7951-64.

(3) Yokoyama, K.; Smith, A. A.; Corzilius, B.; Griffin, R. G.; Stubbe, J. *J. Am. Chem. Soc.* **2011**, *133*, 18420-32.